

EVALUATION OF BIOMASS, INDIAN JUJUBA SEED (IJS) FOR REMOVAL OF CONGO RED

^{1,2}L. Sivaramakrishna, ²M. Sivasankar Reddy, ²M. Jagadeesh,
²W.Y. Wan Zuhairi, ³M.R. Taha and ²A. Varada Reddy

¹School for Environmental Sciences and Natural Resources,

Faculty of Science and Technology, Universiti Kebangsaan Malaysia, 43600 Bangi, Selangor, Malaysia

²Department of Chemistry, Sri Venkateswara University, Tirupati-517 502 (A.P), India

³Department of Civil and Structural Engineering, Universiti Kebangsaan Malaysia, 43600 Bangi, Selangor, Malaysia

Received 2014-01-08; Revised 2014-02-11; Accepted 2014-06-30

ABSTRACT

The present investigation deals with the removal of Congo Red (CR) from aqueous solution by using Indian Jujuba Seed (IJS) as low-cost biosorbent. The effect of pH and size experimental parameters has been investigated using a Batch adsorption technique. Adsorption data were modeled using Langmuir and Freundlich adsorption isotherms. Adsorption kinetics was verified by pseudo-first order, pseudo-second order and intraparticle diffusion models. The kinetic adsorption data fitted the pseudo-second order kinetic model well and also followed the intraparticle diffusion model. The results indicated that IJS could be employed as low-cost biosorbent in wastewater treatment for the removal of CR.

Keywords: Biosorption, Jujuba Seeds (IJS), Congo Red, Kinetic Study

1. INTRODUCTION

Dyes and pigments were used in several industries such as textile, leather tanning, food industries, cosmetics, electroplating, paper and pharmaceuticals. Several classes of synthetic dyes (over 7×10^5 metric tons) are produced worldwide every year for industrial purposes. Above industries generate enormous volumes of wastewater every year. Industries wastewater carrying nearly 5-10% of quantity is released into the ecosystem. The amount of dye in wastewater depends on the type of dye used in industry; it varies from 2% for basic dyes and 10 to 50% for reactive dyes. Dyes containing wastewater discharged into water streams not only contribute negatively to aesthetic value but also causes considerable resistance to biodegradation and may upset aquatic life. Therefore, there is a necessity to treat dyes containing wastewater before their discharge into ecosystem (Rehman *et al.*, 2012).

Now a day's numbers of method are in practice for the removal of dyes from wastewater. Those are solar photo-Fenton degradation, electrochemical degradation, photo catalytic degradation, sonochemical degradation, oxidation and ozonation, integrated chemical-biological degradation, biodegradation, coagulation and flocculation, membrane separation and adsorption. Among the techniques, adsorption is one of the most efficient methods because of its low cost and easy operational conditions (Sivaramakrishna *et al.*, 2012; Yuvaraja *et al.*, 2012; Chowdhury *et al.*, 2011).

To date, in many developed countries, activated carbon is the most widely used adsorbent for dye removal, but it is too expensive. Hence, removal of pollutants from the wastewater remains a challenge to the researchers. The main aim of this study is, to introduce a viable alternative to the commercial activated carbons.

Various non-conventional adsorbents have been attempted and used for the removal of CR from the

Corresponding Author: L. Sivarama Krishna, School for Environmental Sciences and Natural Resources, Faculty of Science and Technology, Universiti Kebangsaan Malaysia, 43600 Bangi, Selangor, Malaysia and Department of Chemistry, Sri Venkateswara University, Tirupati - 517 502 (A.P), India Tel: +91-9441408851

industrial wastewater. A large number of non-conventional adsorbents such as raw pine and acid treated pine cone powder (Dawood and Sen, 2012.), wheat straw (Zhao *et al.*, 2014), eggshells (Saha *et al.*, 2012), natural coagulants (Patel and Vashi 2012), bael shell (Ahmad and Kumar, 2010), cattail root (Hu *et al.*, 2010), Raphanus sativus peel (Abbas *et al.*, 2011), natural coagulants (Surjana seed powder (SSP), maize seed powder (MSP) and chitosan) (Patel and Vashi, 2012), pomelo fruit peel wastes (Jayarajan *et al.*, 2011) and macauba palm (*Acrocomia aculeata*) cake (Vieira *et al.*, 2012) have been used for the removal of CR from aqueous solutions.

This study describes the feasibility of removal of a cationic dye-Congo red from aqueous solutions by using IJS as a new low-cost biosorbent. Batch adsorption experiments were achieved out as a function of biosorbent dosage, contact time, effect pH of dye solution and size effect of adsorbent. The Langmuir and Freundlich isotherms models, kinetics adsorption are also studied.

2. MATERIALS AND METHODS

2.1. Preparation of Biosorbent and Adsorbate Solution

The biomass of Indian Jujuba seed were collected from somayajulapally one of the author native places, these seeds were washed with water and shade dried. The dried material was crushed, powdered and used as biosorbent. These biosorbent was shown in **Fig. 1**.

The solutions of Congo red were prepared by dissolving appropriate amounts of dry powdered dye stuff in distilled water. Stock solution of 1000 mg L⁻¹ was prepared by dissolving accurate quantity of the dye in double distilled water. The working solution was obtained by dilution of a stock solution that was prepared earlier to desire concentration.

2.2. Experimental Section

The primary adsorption test was carried out, to calculate the percentage of CR dye removal. Batch adsorption experiments were carried out by adding a fixed amount of IJS (0.05 g) into 50 mL screw type Erlenmeyer flasks containing 25 mL of CR dye solution (50 mg L⁻¹). The conical flasks then were placed in a shaking thermostatic Julabo water bath shaker at 180 rpm at 35°C. The initial and equilibrium

dye concentrations were determined by absorbance measurement using a Chemito UV-Vis spectrophotometer at 497 nm. It was then computed into dye concentration using a standard calibration curve. The same procedure mentioned above was used to study the effect of different parameters.

The amount of sorption at time t and at equilibrium time and the percentage of dye removal were calculated following Equation 1 and 2:

$$q_t = [(C_0 - C_t)V] / W \quad (1)$$

where, C₀ and C_t (mg L⁻¹) are concentrations of dye at initial and at any time t, respectively, V is the volume of the solution (L) and W is the mass of dry adsorbent used (g).

The dye removal percentage is to be calculated as follows:

$$\text{Removal percentage} = [(C_0 - C_e) / C_0] \times 100 \quad (2)$$

where, C_e is the equilibrium concentration in solution (mg L⁻¹).

2.3. Point of Zero Charge (pH_{PZC})

The zero surface charge characteristics of the IJS were determined, using the solid addition method (Sivaramakrishna *et al.*, 2012). Forty milliliters of 0.1M KNO₃ solution was transferred to a series of 100 mL Stoppard conical flasks. The pH_i values of the solutions were roughly adjusted between 2 and 12 by adding either 0.1N HCl or NaOH and measured by using pH meter (Systronics pH system 361 Model, India). The total volume of the solution in each flask was exactly adjusted to 50 mL by adding the KNO₃ solution of the same strength. The pH_i of the solutions were then accurately noted. 0.05 gm of IJS was added to each flask and the flask was securely capped immediately. The suspensions were then kept shaking for 24 h and allowed to equilibrate for 0.5 h. The final pH values of the supernatant liquid were noted. The difference between the initial and final pH (pH_f) values (ΔpH) was plotted against the pH_i. The point of intersection of the resulting curve with abscissa, at which pH = 0, gave the pH_{PZC}. It is observed from **Fig. 2** that the surface charge of the IJS around pH 7 is zero. Hence, the pH_{PZC} at point of zero charge of the IJS is 7.



Fig. 1. Pieces of Jujuba seeds

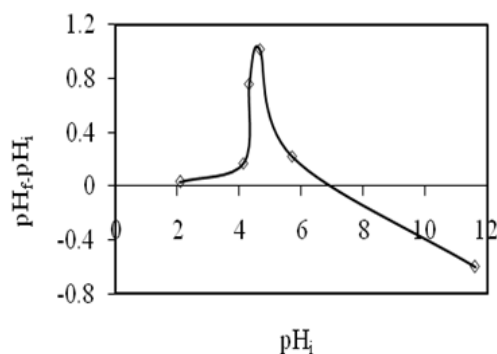


Fig. 2. Point of zero charge of IJS

2.4. Batch Adsorption Studies

In the present study, batch adsorption experiments were carried out by agitating 50 mg of adsorbent, IJS with 25 mL of dye solutions of concentration is 50mg L⁻¹, in a 50 mL screw type Erlenmeyer flask at room temperature (30±1°C). A good contact is made between adsorbent and dye by agitating at 180 rpm in a Julabo shaking water bath. Dye concentration is determined spectrophotometrically by monitoring the absorbance at 497 nm using Chemito UV-VIS Spectrophotometer and two 1 cm cells. The wavelength of the maximum absorbance for dye was selected and λ_{max} value is 497 nm. The pH of dye solutions was determined using pH meter (Systronics pH system 361 model, India). The samples were withdrawn from the shaker at pre-determined time intervals and the dye solution was separated from the adsorbent by centrifugation at 10,000 rpm for 20 min. The absorbance of supernatant solution is measured to Equation 1 and 2.

2.5. Batch Kinetic Studies

2.5.1. Effect of pH

The effect of pH studied at three different pHs of 5, 6.95 and 9. The pH is adjusted by using NaOH and HCl solutions of different concentrations depending on the requirement. In this study, 25 ml of different pH adjusted dye solution of 50 mg L⁻¹ is taken in a screw type Erlenmeyer flask and agitated at 180 rpm, with 0.05 g of <53 μm of IJS at temperature, 30±1°C. The samples are withdrawn from the shaker at pre-determined time intervals and the dye was separated from the adsorbent by centrifugation at 10,000 rpm for 20 min. The absorbance of supernatant solution is measured. The amount of CR adsorbed is calculated by using Equation 1.

2.5.2. Effect of size

The effect of size studied at different sizes of IJS like <53 μm, >53<75 μm, >75<90 μm and >90<150 μm. In this study, 25 mL of dye solution of 50 mg L⁻¹ is taken in a screw type Erlenmeyer flask and agitated at 180 rpm, with different size of IJS at temperature, 30±1°C. The dye solution pH is maintained at 6.95 in this study. The samples are withdrawn from the shaker at pre-determined time intervals and the dye solution is separated from the adsorbent by centrifugation at 10,000 rpm for 20 min. The absorbance of supernatant solution is measured. The amount of CR adsorbed is calculated by using Equation 1.

2.6. Theory of Adsorption Kinetics and Isotherms

2.6.1. Kinetic models

The Lagergren's Pseudo-First-Order model (PFO) (Equation 3) and Pseudo-Second-Order (PSO) model (Equation 4) (Sivaramakrishna *et al.*, 2012) have been widely used to predict sorption kinetics. The PFO equation is generally applicable over the initial stage of the adsorption processes whereas the PSO equation predicts the behavior over the whole range of adsorption. These two models are used in this study to fit the experimental data:

$$\log(q_e - q_t) = \log q_e - (k_1 / 2.303)t \quad (3)$$

$$t / q_t = (1 / k_2 q_e^2) + (1 / q_e)t \quad (4)$$

where, k₁ (min⁻¹) is the rate constant of PFO adsorption and k₂ (g mg⁻¹ min⁻¹) is the rate constant

of PSO adsorption. q_e , amount of dye adsorbed on adsorbent at equilibrium.

2.6.2. Intra-Particle Diffusion Model

In order to investigate the mechanism of the CR adsorption onto IJS, intra-particle diffusion based mechanism is studied. The most commonly used technique for identifying the mechanism involved in the adsorption process is by hitting an intra-particle diffusion plot. It is an empirically found functional relationship, common to the most adsorption processes, where uptake varies almost proportionally with $t^{0.5}$ rather than with the contact time t . According to the theory proposed by Weber and Morris (Sivaramakrishna *et al.*, 2012):

$$q_t = k_{pi} t^{0.5} + C_i \quad (5)$$

where, k_{pi} ($\text{mg g}^{-1} \text{min}^{-0.5}$), the rate parameter of stage i , is obtained from the slope of the straight line of q_t versus $t^{0.5}$ where as C_i is the intercept of the plot which gives an idea about the thickness of the boundary layer.

Langmuir isotherm model was applied to describe the adsorption of CR. It represented by the following equation:

$$(C_e / q_e) = (1 / Q_{max} K_L) + (C_e / Q_{max}) \quad (6)$$

where, Q_{max} is the maximum adsorption capacity of IJS (mg g^{-1}) and K_L is the Langmuir constant related to the adsorption energy (L mg^{-1}).

Freundlich isotherm model is also applied to describe the adsorption of CR. Linearized in logarithmic form of Freundlich isotherm model equation is represented by:

$$\log q_e = \log K_F + (1/n) \log C_0 \quad (7)$$

where, K_F is the Freundlich constant and '1/n' is the heterogeneity factor.

3. RESULTS

3.1. Effect of Contact Time

The adsorption of CR on IJS was studied at different CR pHs ranges (5, 6.95 and 9) and different sizes (<53 μm , >53<75 μm , >75<90 μm and >90<150 μm) **Fig. 2 and 3** shows the result for effect of pH and sizes on adsorption of CR onto IJS at $30 \pm 1^\circ\text{C}$.

3.1.1. Effect of pH

The effect of pH on the amount of dye removal is kinetically studied at three different pHs of 5, 6.95 and 9.

For understanding the effect of pH on the adsorption of CR on IJS, the PFO and PSO kinetic models were used to fit the experimental data obtained in these experiments. Using Equation 3 and 4, a $\log(q_e - q_t)$ versus t is plotted at different pH of CR solutions (**Fig. 5**). The PFO model data do not fall on straight lines indicating that this model is less appropriate. The Lagergren first-order rate constant (k_1) and calculated from the model are presented in **Table 1** along with the corresponding with correlation coefficients.

The experimental kinetic data is further analyzed using the pseudo-second-order model. By plotting t/q_t against t for different initial CR concentrations (**Fig. 6**), a straight line is obtained in all cases and using Equation (4), the PSO constant (k_2) and q_e values were determined from the plots. The values of correlation coefficient are very high ($R^2 > 0.999$) and the theoretical $q_{e \text{ cal}}$ values obtained from this model are closer to the experimental $q_{e \text{ exp}}$ values at different pHs (**Table 1**). It is important to note that for the PFO model, the correlation coefficient obtained in this study, $R^2 < 0.93$ at different pHs of CR solution, is lower as compared to the correlation coefficient obtained from the pseudo-second order model. Moreover, from **Table 1**.

3.1.2. Effect of Size

The adsorption kinetic studies are also performed at three different particle sizes at adsorption dose of 2.0 g L^{-1} of IJS. For understanding the effect of size of IJS on the adsorption of CR on IJS, the PFO and PSO kinetic models are used to fit the experimental data obtained in these experiments. Using Equation 3 and 4, a $\log(q_e - q_t)$ versus t is plotted at different size of adsorbent (**Fig. 7**). The PFO model data do not fall on straight lines indicating that this model is less appropriate. The Lagergren first-order rate constant (k_1) was calculated from the model and the results are presented in **Table 3** along with corresponding correlation coefficients.

3.2. Kinetic Study

The kinetic results are analyzed by using the intraparticle diffusion model also. Weber and Moris model (Sivaramakrishna *et al.*, 2012) was used through Equation 5 to investigate intra-particle diffusion mechanism by plotting a graph between q_t versus $t^{0.5}$ (**Fig. 8**). At least three regions observed that represent boundary layer diffusion, followed by intra-particle diffusion in macro, meso and micro pores. These three regions are followed by a horizontal line representing the system at equilibrium.

Table 1. Pseudo-first-order and pseudo-second-order rate constants at 30°C and different pH of CR solutions

pH	$q_{e\text{ exp}}$ (mg g^{-1})	Pseudo-first-order model			Pseudo-second-order model		
		K_1 (min^{-1})	$q_{e\text{ cal}}$ (mg g^{-1})	R^2	K_2 (min^{-1})	$q_{e\text{ cal}}$ (mg g^{-1})	R^2
5	20.8804	0.0092	22.2867	0.9300	0.0059	21.0214	0.9980
6.95	19.9197	0.0092	21.2631	0.9500	0.0101	20.0020	0.9990
9	20.8242	0.0115	21.5038	0.9270	0.0146	20.8812	0.9990

Table 2. Intra-particle diffusion constants for different pHs of CR solution at 30°C

Linear Portion ↓	Constants ↓	pH5	pH6.95	pH9
First	K_{p1} ($\text{mg g}^{-1} \text{min}^{-0.5}$)	0.3932	1.5130	0.1756
	C_1 (mg g^{-1})	16.1270	6.8721	16.5510
	R^2	0.9397	0.9747	0.9883
Second	K_{p2} ($\text{mg g}^{-1} \text{min}^{-0.5}$)	0.3256	0.3802	0.1918
	C_2 (mg g^{-1})	16.6140	14.7120	17.6500
	R^2	0.9485	0.9910	0.9740
Third	K_{p3} ($\text{mg g}^{-1} \text{min}^{-0.5}$)	0.1276	0.1703	0.1719
	C_3 (mg g^{-1})	18.0520	16.9840	17.7400
	R^2	0.8688	0.9858	0.9520
Fourth	K_{p4} ($\text{mg g}^{-1} \text{min}^{-0.5}$)	0.1005	-	-
	C_4 (mg g^{-1})	19.2000	-	-
	R^2	0.7958	-	-

Table 3. Pseudo-first-order and pseudo-second-order rate constants at 30°C and different sizes of IJS

Size	$q_{e\text{ exp}}$ (mg g^{-1})	Pseudo-first-order model			Pseudo-second-order model		
		K_1 (min^{-1})	$q_{e\text{ cal}}$ (mg g^{-1})	R^2	K_2 (min^{-1})	$q_{e\text{ cal}}$ (mg g^{-1})	R^2
<53 μm	19.9197	0.0138	20.2395	0.9500	0.0059	20.0607	0.9990
<53 >75 μm	19.7290	0.0161	16.4537	0.8430	0.0101	16.4059	0.9980
<75 >90 μm	9.7295	0.0115	10.0470	0.9070	0.0148	9.7863	0.9990
<90 >150 μm	8.2022	0.0048	10.9524	0.8690	0.0353	8.2258	0.9980

Table 4. Intra-particle diffusion constants for different sizes of IJS at 30°C

Linear Portion ↓	Constants ↓	<53 μm	>53<75 μm	>75<90 μm	>90<150 μm
First	K_{p1} ($\text{mg g}^{-1} \text{min}^{-0.5}$)	1.5130	1.610	0.871	0.461
	C_1 (mg g^{-1})	6.8721	5.146	3.154	2.919
	R^2	0.9747	0.989	0.967	0.993
Second	K_{p2} ($\text{mg g}^{-1} \text{min}^{-0.5}$)	0.3802	0.282	0.395	0.228
	C_2 (mg g^{-1})	14.7120	12.633	5.671	4.055
	R^2	0.9910	0.949	0.867	0.930
Third	K_{p3} ($\text{mg g}^{-1} \text{min}^{-0.5}$)	0.1703	0.020	0.087	0.067
	C_3 (mg g^{-1})	16.9840	15.120	8.173	5.374
	R^2	0.9858	0.988	0.989	0.985
Fourth	K_{p4} ($\text{mg g}^{-1} \text{min}^{-0.5}$)	-	-	-	-
	C_4 (mg g^{-1})	-	-	-	-
	R^2	-	-	-	-

At the beginning of adsorption, there is a linear region representing the rapid surface loading, followed by the second linear region representing pore diffusion and finally a horizontal linear region representing the equilibrium. The Microsoft Excel 2003 software package is used to analyze various regions available in the graph and results of linear

regression are shown in **Table 2 and 4** for various sizes of IJS and different pH of solutions. The intra-particle diffusion parameter, k_{pi} , is determined from the slope of each region while the intercept of each region is proportional to the boundary-layer thickness. The calculated values of k_{pi} and the intercept, C, for all the linear regions are shown in **Table 2 and 4**.

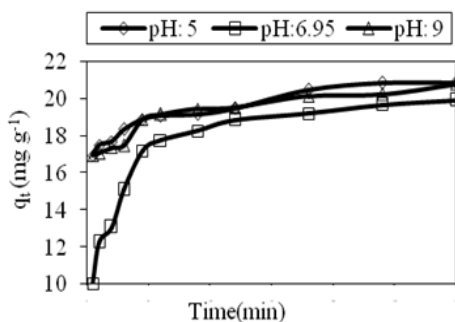


Fig. 3. Effect of pH on CR adsorption

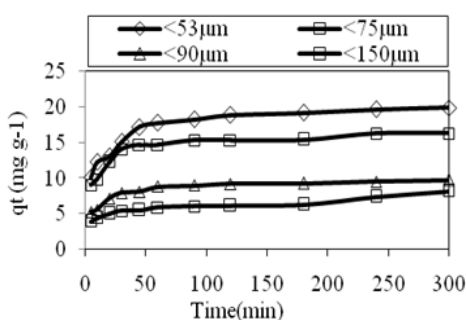


Fig. 4. Effect of size on CR adsorption

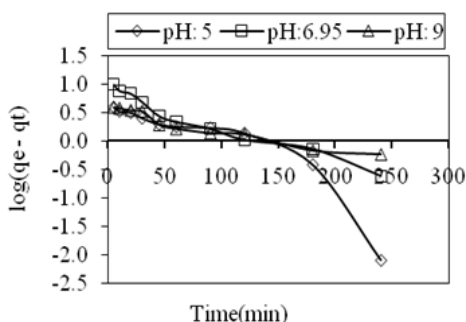


Fig. 5. Pseudo-first-order model for CR onto IJS for different pHs

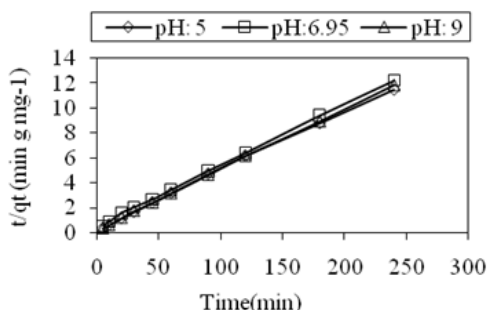


Fig. 6. Pseudo-second-order model for CR onto IJS for different pHs

4. DISCUSSION

In this study dye uptake was rapid for the first 60 minutes and thereafter proceeds at a slower rate and finally attains saturation. **Figure 3 and 4** indicates that an increase in CR pH leads to decrease in the adsorption of CR on IJS. The equilibrium adsorption decreases from 20.8804 to 20.8242 mg g⁻¹ and 19.9197 to 8.2022 mg g⁻¹ for pH and size respectively. However, the experimental data is measured at 300 min to be sure that full equilibrium is attained. Data on the adsorption kinetics of CR by various biosorbent have shown similar range of adsorption rates. Hu *et al.* (2010) and Sivaramakrishna *et al.* (2012) studied the adsorption of CR on cattail root (Hu *et al.*, 2010) and Jujuba seeds (Sivaramakrishna *et al.*, 2012) and both studies reported that the equilibrium was reached in 3 h.

The values of correlation coefficient are very high ($R^2 > 0.999$) and the theoretical $q_{e\text{ cal}}$ values obtained from this model are closer to the experimental $q_{e\text{ exp}}$ values at different pHs (**Table 1**). It is important to note that for the PFO model, the correlation coefficient obtained in this study, $R^2 < 0.93$ at different pHs of CR solution, is lower as compared to the correlation coefficient obtained from the PSO model. Moreover, from **Table 1**, it can be seen that the experimental values of $q_{e\text{ exp}}$ are not in good agreement with theoretical values calculated ($q_{e\text{ cal}}$) from the PFO equation. Therefore, it can be concluded that the PSO kinetic model provides a better correlation for the adsorption of CR on IJS at different pHs of CR solution compared to the PFO model. The effect of pH of acid brown dye solution on the activated carbon (solid waste generated in leather industry) is studied (Sekaran *et al.*, 1995) it is similar to this studies.

The experimental kinetic data are further analyzed using the PSO model. By plotting t/q_t against t for different initial CR concentrations (**Fig. 8**), a straight line is obtained in all cases and using Equation 4, the PSO rate constant (k_2) and q_e values are determined from the plots. The values of correlation coefficient are very high ($R^2 > 0.998$) and the theoretical $q_{e\text{ cal}}$ values obtained from this model were closer to the experimental $q_{e\text{ exp}}$ values at different sizes of IJS (**Table 3**). It is important to note that for the PFO model, the correlation coefficient obtained in this study, $R^2 < 0.843$ at different sizes of IJS, which is lower as compared to the correlation coefficient obtained from the PSO model. Moreover, from **Table 3**, it can be seen that the experimental values of $q_{e\text{ exp}}$ are not in good agreement with theoretical values calculated ($q_{e\text{ cal}}$) from the PFO equation. Therefore, it can be concluded that the PSO kinetic model provided a better correlation for the adsorption of CR on IJS at different sizes of IJS compared to the PFO model.

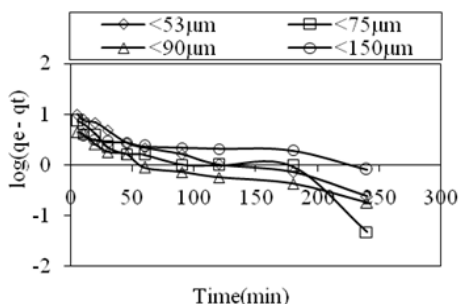


Fig. 7. Pseudo-first-order model for CR onto IJS for different sizes

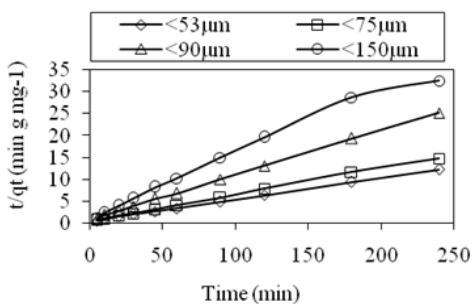


Fig. 8. Pseudo-second-order model for CR onto IJS for different sizes

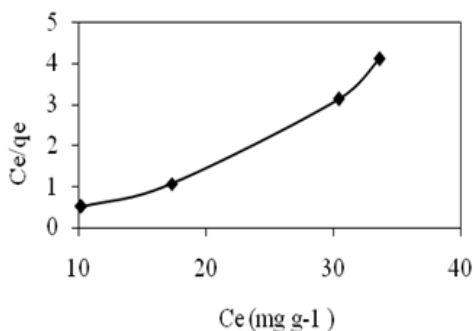


Fig. 9. Langmuir isotherm of CR onto IJS for different sizes

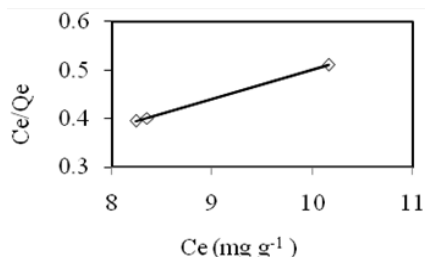


Fig. 10. Langmuir isotherm of CR onto IJS for different pHs

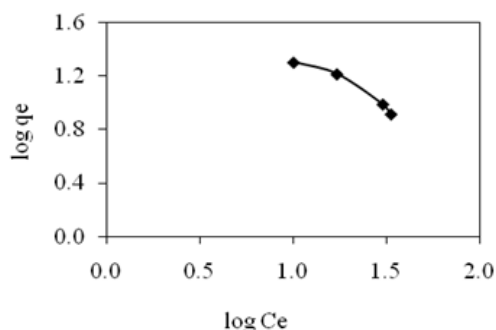


Fig. 11. Freundlich isotherm of CR onto IJS for different sizes

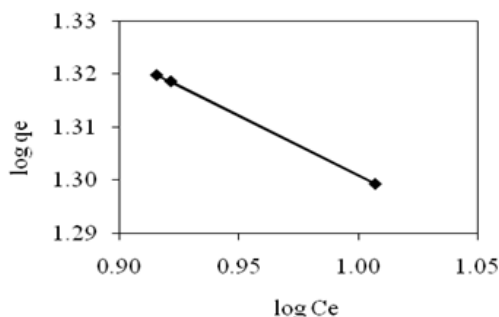


Fig. 12. Freundlich isotherm of CR onto IJS for different pHs

The effect of size of activated carbon on the removal of acid brown dye on activated carbon (solid waste generated in leather industry) was studied (Sekaran *et al.*, 1995) and size of activated clay on the removal of basic blue 18, basic red 46 and basic yellow 28 by activated clay (Hsu *et al.*, 1997) similar to this study.

4.1. Equilibrium Modeling

The adsorption of CR on IJS was modeled with the Langmuir and Freundlich adsorption isotherms. The details of the Langmuir and Freundlich isotherms are given in Equation 6 and 7 and their respective plots are shown in **Fig. 9 to 12**, respectively. The values of the Langmuir and Freundlich constants obtained in this study are presented in **Table 5**. Both, Langmuir and Freundlich models are well suited for the experimental data of CR on IJS, as per the coefficients of correlation. Negative values for the Langmuir and Freundlich isotherm constants in **Table 5** indicate the inadequacy of the isotherm model to explain the sorption process. These kind of negative values are available in the literature (Rabinson *et al.*, 2012).

Table 5. Langmuir and Freundlich constants for different sizes and pH

Parameters	Langmuir constants		R ²	Freundlich constants		
	Q _{max} (mg g ⁻¹)	K _L (L mg ⁻¹)		K _F	n	R ²
Size (µm)	5.6497	-0.4854	0.9820	29.8000	-1.0050	0.9990
pH	16.6670	-9.9010	1.0000	33.6000	-4.4444	1.0000

5. CONCLUSION

The present study focuses on the biosorption of CR dye from aqueous solution using IJS. The adsorption characteristics have been examined by contact time, pH effect and effect of biosorbent size. The maximum removal of CR was observed at pH 5.0. The biosorption of CR onto IJS was found to increase with decrease in biosorbent size. Based on correlation coefficient (r^2 value), the experimental data was best fitted with Langmuir model than Freundlich isotherm model. The suitability of PFO, PSO and intraparticle diffusion kinetic models for the biosorption of CR onto IJS was also discussed. Kinetic data follows the PSO kinetic model. Intraparticle diffusion model proves that pore diffusion plays major role in the dye biosorption. The results showed the possibility of IJS for dye removal from aqueous solution as an alternative for most costly used biosorbent.

6. ACKNOWLEDGEMENT

The authors are thankful to Universiti Kebangsaan Malaysia for to conduct research work. L. Sivaramakrishna is thanks to Universiti Kebangsaan Malaysia for financial support.

7. REFERENCES

- Abbas, S.M.A., N. Belhocine, A.A. ElGanainy and M. Horton, 2011. Historical patterns and dynamics of public debt-evidence from a new database. *IMF Econom. Rev.*, 59: 717-742.
- Ahmad, R. and R. Kumar, 2010. Adsorptive removal of Congo red dye from aqueous solution using bael shell carbon. *Applied Surf. Sci.*, 257: 1628-1633. DOI: 10.1016/j.apsusc.2010.08.111
- Chowdhury, Z.Z., S.M. Zain, R.A. Khan and A.A. Ahmed, 2011. Equilibrium kinetics and isotherm studies of Cu (II) adsorption from waste water onto alkali activated oil palm ash. *Am. J. Applied Sci.*, 8: 230-237. DOI: 10.3844/ajassp.2011.230.237
- Dawood, S. and T.K. Sen, 2012. Removal of anionic dye Congo red from aqueous solution by raw pine and acid-treated pine cone powder as adsorbent: Equilibrium, thermodynamic, kinetics, mechanism and process design. *Water Res.*, 46: 1993-1946. DOI: 10.1016/j.watres.2012.01.009
- Hsu, Y.C., C.C. Chiang and M.F. Yu, 1997. Adsorption behavior of basic dyes on activated clay. *J. Sep. Sci. Tech.*, 32: 2513-2534. DOI: 10.1080/01496399708000783
- Hu, Z., H. Chen, F. Ji and S. Yuan, 2010. Removal of Congo red from aqueous solution by cattail root. *J. Hazard. Mat.*, 173: 292-297. DOI: 10.1016/j.jhazmat.2009.08.082
- Jayarajan, M., R. Arunachalam and G. Annadurai, 2011. Use of low cost nano-porous materials of pomelo fruit peel wastes in removal of textile dye. *Res. J. Environ. Sci.*, 5: 434-443. DOI: 10.3923/rjes.2011.434.443
- Patel, H. and R.T. Vashi, 2012. Removal of Congo Red dye from its aqueous solution using natural coagulants. *J. Saudi Chem. Society*, 16: 131-136. DOI: 10.1016/j.jscs.2010.12.003
- Rabinson, T., B. Chandran and P. Nigam, 2002. Removal of dyes from a synthetic textile dye effluent by biosorption on apple pomace and wheat straw. *Water Res.*, 36: 2824-2830. DOI: 10.1016/S0043-1354(01)00521-8
- Rehman, M.S.U., I. Kim and J.I. Jon Han, 2012. Adsorption of methylene blue dye from aqueous solution by sugar extracted spent rice biomass. *Carbo. Poly.*, 90: 1314-1322. PMID: 22939346
- Saha, P.D., S. Chowdhury, M. Mondal and K. Sinha, 2012. Biosorption of Direct Red 28 (Congo Red) from aqueous solutions by eggshells: Batch and column studies. *Separ. Sci. Technol.*, 47: 112-123. DOI: 10.1080/01496395.2011.610397
- Sekaran, G., K.A. Shanmugasundaram, K.V. Mariappan and M. Raghavan, 1995. Adsorption of dyes by buffing dust of leather industry. *Ind. J. Chem. Tech.*, 2: 311-316.

- Sivaramakrishna, L., M.C.S. Reddy and A.V. Reddy, 2012. The use of an Agricultural Waste Material, Jujuba Seeds for the Removal of anionic dye (Congo Red) from Aqueous Medium. *J. Hazard. Materials*, 203-204: 118-127. DOI: 10.1016/j.jhazmat.2011.11.083
- Vieira, S.S., Z.M. Magriotios, N.A.V. Santos, M.G. Cardoso and A.A. Saczk, 2012. Macauba palm (*Acrocomia aculeata*) cake from biodiesel processing: An efficient and low cost substrate for the adsorption of dyes. *Chem. Eng. J.*, 183: 152-161. DOI: 10.1016/j.cej.2011.12.047
- Yuvaraja, G., M.V. Subbaiah and A. Krishnaiah, 2012. *Caesalpinia bonducella* leaf powder as biosorbent for Cu(II) Removal from aqueous environment: Kinetics and isotherms. *Ind. Eng. Chem. Res.*, 51: 11218-11225. DOI: 10.1021/ie203039m
- Zhao, B., Y. Shang, W. Xiao, C. Dou and R. Han, 2014. Adsorption of Congo red from solution using cationic surfactant modified wheat straw in column model. *J. Environ. Chem. Eng.*, 2: 40-45. DOI: 10.1016/j.jece.2013.11.025